

Ferromagnetism in $\text{Ga}_{1-x}\text{Mn}_x\text{P}$: evidence for inter-Mn exchange mediated by localized holes within a detached impurity band

M. A. Scarpulla¹, B. L. Cardozo¹, W. M. Hlaing Oo², M. D. McCluskey², and O. D. Dubon^{1,*}

¹*Department of Materials Science & Engineering, University of California at Berkeley and Lawrence Berkeley National Laboratory, Berkeley, California 94720*

²*Department of Physics, Washington State University, Pullman, WA 99164-2814*

ABSTRACT

We demonstrate that in ferromagnetic $\text{Ga}_{1-x}\text{Mn}_x\text{P}$ exchange is mediated by holes localized in a Mn-derived band. For $x < 0.06$, infrared absorption and photoconductivity spectra indicate the presence of a Mn impurity band which is not merged with the valence band. At temperatures above T_C (≤ 65 K) electrical transport is dominated by excitation across this energy gap while nearest neighbor hopping dominates below T_C . Magnetization measurements reveal a moment of $3.5 \mu_B$ per substitutional Mn, while the large anomalous Hall signal unambiguously demonstrates that the ferromagnetism is carrier-mediated.

PACS Numbers: 75.50.Pp, 72.60.+g, 75.47.-m, 73.50.Pz

* Corresponding author: oddubon@socrates.berkeley.edu

Diluted magnetic semiconductors (DMSs) are materials where a few atomic percent of a magnetic element is added to a non-magnetic semiconductor. Because of their unique combinations of magnetic and semiconducting properties and their potential for use as both injection sources and filters for spin-polarized carriers, these materials have been suggested for use in spin-based electronics, or *spintronics*. The manipulation of carrier spin provides an additional degree of freedom in the operation of devices for use in energy-efficient electronics as well as for information storage and processing. The discovery of ferromagnetism in the III-Mn-V systems $\text{In}_{1-x}\text{Mn}_x\text{As}$ and $\text{Ga}_{1-x}\text{Mn}_x\text{As}$ [1,2] heralded more than a decade of intense experimental and theoretical research [3-6].

In order for DMSs to display ferromagnetic ordering, long-range exchange mechanisms must operate because of the large average distances between the localized magnetic moments. There is reasonable consensus that the indirect inter-Mn exchange in $\text{Ga}_{1-x}\text{Mn}_x\text{As}$ – the most thoroughly studied and well-understood ferromagnetic III-Mn-V system - and other ferromagnetic DMSs such as $\text{Zn}_{1-x}\text{Mn}_x\text{Te}$ [7] and $\text{Ga}_{1-x}\text{Mn}_x\text{Sb}$ [8] is mediated by holes in extended or weakly localized states. In particular, the model put forth by Dietl *et al.* has been successful in accounting for many of the properties of these systems [9]. The weakly localized character of holes in $\text{Ga}_{1-x}\text{Mn}_x\text{As}$ is due to the formation of an impurity band from Mn acceptor states (binding energy ~ 110 meV in the dilute Mn concentration limit) that merges with the GaAs valence band [10]. Manganese doped GaP represents a case of much stronger hole localization due to the larger binding energy (~ 400 meV) of Mn acceptors [11]. A recent bandstructure calculation has predicted that a spin-polarized Mn impurity band may overlap only slightly with the valence band for an ordered alloy of $\text{Ga}_{0.94}\text{Mn}_{0.06}\text{P}$ [12]. The extreme example of

localization of exchange-mediating carriers is provided by $\text{In}_{1-x}\text{Mn}_x\text{As}$ grown by metalorganic vapor phase epitaxy, in which isolated Mn dimers and trimers are ferromagnetically coupled resulting in a Curie temperature (T_C) of 333 K [13]. Within this spectrum of localization, $\text{Ga}_{1-x}\text{Mn}_x\text{P}$ represents an important medium for investigating carrier-mediated ferromagnetism.

In this work, we present experimental evidence that in $\text{Ga}_{1-x}\text{Mn}_x\text{P}$ ferromagnetism is mediated by localized holes residing in a Mn-derived impurity band that is distinct from the valence band. The measurement of a large anomalous Hall signal reflecting the sample magnetization and a dramatic enhancement of magnetoresistance near T_C unambiguously demonstrate that the ferromagnetism in these samples is mediated by the same holes responsible for electrical conduction. Despite the strongly insulating nature of these films, samples with $x \sim 0.06$ exhibit T_C s above 60 K. Previous reports [14] have indicated that ferromagnetism exists in polycrystalline GaP-based layers grown with Mn; however, there have been no reports of transport measurements establishing that the observed ferromagnetism was indeed due to a carrier-mediated phase.

As in other III-V semiconductors, the solubility of Mn in GaP is anomalously high compared to other 3d transition metals ($3 \times 10^{19} / \text{cm}^3$) [11]. Nevertheless, non-equilibrium growth techniques are still required to achieve the $10^{21} / \text{cm}^3$ concentrations at which carrier-mediated ferromagnetism is expected. Samples for this study were produced using ion implantation into GaP followed by pulsed-laser melting (PLM). We have used this process very successfully to synthesize $\text{Ga}_{1-x}\text{Mn}_x\text{As}$ layers with T_C up to 137 K [15-18], which compares well with the maximum reported T_C of 175 K [19] for layers grown by molecular beam epitaxy. Briefly, an n-type GaP (001) wafer was implanted with 50

keV Mn⁺ to a dose of $2 \times 10^{16}/\text{cm}^2$. Each implanted sample measuring roughly 5 mm on each edge was irradiated in air with a single $0.3\text{-}0.4 \text{ J}/\text{cm}^2$ pulse from a KrF excimer laser ($\lambda = 248 \text{ nm}$). The laser has a roughly triangular temporal pulse shape with FWHM = 19 ns and is homogenized to a spatial uniformity of $\pm 5 \%$ by a crossed-cylindrical lens homogenizer. Extended etching in concentrated HCl was used to remove a poorly-regrown layer [16] from the surface. Ion channeling techniques were used to determine total Mn doses and substitutional fractions, while secondary ion mass spectrometry (SIMS) was used to determine Mn depth profiles [15-18].

Figure 1 presents the in-plane low-field (50 Oe) magnetization of two $\text{Ga}_{1-x}\text{Mn}_x\text{P}$ films. For a $\text{Ga}_{0.94}\text{Mn}_{0.06}\text{P}$ sample irradiated at $0.4 \text{ J}/\text{cm}^2$ (solid line) a nearly linear dependence of magnetization on temperature up to its T_C of 60 K is observed. Samples from the same Mn implantation irradiated between $0.3\text{-}0.35 \text{ J}/\text{cm}^2$ show a maximum T_C of 65 K while $\text{Ga}_{0.97}\text{Mn}_{0.03}\text{P}$ films display T_C up to 23 K [16]. At 5 K and in a field of 5 T, the magnetization of the $\text{Ga}_{0.94}\text{Mn}_{0.06}\text{P}$ film saturates at a value corresponding to $3.5 \mu_B$ per *substitutional* Mn and $2.3 \mu_B$ per *total* Mn. The dashed line in Fig. 1 presents data from a sample compensated with Te donors. We interpret the decrease in magnetization and T_C as being due to the reduced hole concentration resulting from the partial compensation of Mn acceptors by Te donors. These magnetic characteristics are consistent with the ferromagnetism in our $\text{Ga}_{1-x}\text{Mn}_x\text{P}$ films being due to a carrier-mediated ferromagnetic phase.

The main panel of Fig. 2 presents the Hall resistance as a function of magnetic field for a sample having a T_C of 65 K. The anomalous component has the same sign as is observed in $\text{Ga}_{1-x}\text{Mn}_x\text{As}$ and comprises a significant portion of the signal even well

above T_C (e.g. at 100 K). The magnitude of the anomalous Hall resistivity increases nearly linearly with decreasing temperature below T_C , reflecting the magnetization shown in Fig. 1. The inset of Fig. 2 shows that the magnetoresistivity at 7 T reaches its largest magnitude of -48 % at the T_C of 65 K. These transport characteristics reflecting the intimate, causal relationship between hole transport and ferromagnetism are observed in other III-V ferromagnetic semiconductor random alloys [7,8] as well as in manganites [20].

The circles in Fig. 3 represent the sheet resistivity of the same sample from Fig. 2 as a function of inverse temperature. The sample is clearly non-metallic and its resistivity is well described by a model of two parallel thermally-activated processes:

$$\rho(T)^{-1} = (C_1 \exp\{E_1/k_B T\})^{-1} + (C_2 \exp\{E_2/k_B T\})^{-1} \quad (1)$$

with the high- and low-temperature activation energies $E_{1,2}$ and the pre-exponential factors $C_{1,2}$ as fitting parameters. Fitting the data to this model gives the high- and low-temperature activation energies as ~ 31 and ~ 6 meV, respectively. This behavior is widely observed in semiconductors doped with hydrogenic impurities to moderate levels below the Mott metal-insulator transition [21]. In such materials doped with acceptors, the high-temperature activation energy is due to transitions from the impurity states to the valence band while the low temperature activation energy results from nearest-neighbor hopping between impurity states. We assign the high-temperature ~ 31 meV activation energy to excitation across a gap between the Mn impurity and valence bands and the 6 meV activation energy to nearest-neighbor hopping within the Mn impurity band. We also note that the change in slope occurs near T_C in these $\text{Ga}_{1-x}\text{Mn}_x\text{P}$ samples, which may

indicate a link between the dominant mechanism of conductivity and the ferromagnetic transition.

We used far-infrared photoconductivity (PC) and infrared (IR) absorption spectroscopy to investigate the Mn impurity band in $\text{Ga}_{1-x}\text{Mn}_x\text{P}$. In PC spectroscopy, excitation of strongly localized holes into extended or weakly localized states results in a change in conductivity that is readily detectable by lock-in techniques with much greater sensitivity than can be achieved with absorption measurements. The solid red line in Fig. 4a shows the IR photoconductivity response from the $\text{Ga}_{0.94}\text{Mn}_{0.06}\text{P}$ sample at 4.2 K while the dashed line is the instrument response, or spectrum of incident light on the sample. All of the gross features of the instrument response are reproduced in the sample PC spectrum with the exception of the region below ~ 26 meV. As the instrument response function has appreciable spectral weight in this region, the absence of sample response in this region is direct evidence of an energy gap across which carriers are optically excited. This gap energy is in good agreement with that deduced from the resistivity data, and together these suggest the existence of a Mn impurity band that is separated from the valence band, as depicted in Fig. 4d.

To further test our hypothesis that the Mn impurity band is not merged with the valence band, we measured the photoconductivity spectra of Te-compensated and $\text{Ga}_{0.97}\text{Mn}_{0.03}\text{P}$ samples. In the $\text{Ga}_{0.97}\text{Mn}_{0.03}\text{P}$ sample, the onset of the PC response is shifted to a higher energy of ~ 47 meV, which is as well in good agreement with the measured activation energy of ~ 53 meV for the high-temperature region of the sample's resistivity. These observations are consistent with a narrowing of the impurity band with decreasing Mn concentration. Figure 4b demonstrates that in the Te compensated sample

the onset of the PC response at 4.2 K is shifted to ~ 70 meV (depicted schematically in Fig. 4d), which is indicative of a shift of the Fermi energy deeper into the Mn band due to a reduction of the hole concentration (i.e., Te donors compensating Mn acceptors). The spectra taken at higher temperatures demonstrate a gradual increase in spectral weight at lower energies and an eventual return of the onset in PC response to near 26 meV. At temperatures above 18.5 K the onset PC response increases in intensity but does not shift to lower energy. These observations are consistent with a thermal redistribution of holes whereby the impurity-band edge states are occupied at 18.5 K.

Figure 4c presents the results of infrared absorption measurements in the photon energy range between 150 and 800 meV on the Te-compensated sample shown in Fig. 4b at 10 K. The spectrum is characterized by a weak, wide feature peaked between 300 - 400 meV and apparently extending to at least 600 meV, which we interpret as resulting from transitions from within the Mn-derived impurity band to the valence band. The center of this peak is near the Mn acceptor ionization energy in GaP of ~ 400 meV. The data have been normalized to the spectrum from a sample which was implanted with Kr^+ and irradiated under identical laser conditions; such normalization is used to remove optical absorption features resulting from multiphonon absorption by GaP as well as sample processing but not directly related to the presence of Mn. The sharp dips in the spectrum reflect non-idealities in the normalization, which also obscure the absorption spectrum below ~ 150 meV. Nevertheless, the data clearly indicate a rapid decrease in the impurity band density of states approaching the valence band edge, consistent with the PC results.

The presence of an impurity band separated from the valence band by 26-31 meV intuitively suggests that $\text{Ga}_{0.94}\text{Mn}_{0.06}\text{P}$ should be highly conducting at room temperature. However, we estimate that the room-temperature free-hole concentration is in the range of $10^{18} /\text{cm}^3$, reflecting the small impurity-band density of states near the impurity band edge. We have found good agreement between our observations and models of carrier statistics predicting $10^{18} /\text{cm}^3$ free hole concentrations having symmetric impurity bands of various shapes centered on 360 meV and separated by a gap of 25 meV from the valence band edge, as indicated by the PC and IR absorption measurements. This concentration is 2-3 orders of magnitude less than the free-hole concentrations observed in ferromagnetic $\text{Ga}_{1-x}\text{Mn}_x\text{As}$ having comparable values of T_C .

A fundamental unresolved issue in the understanding of III-Mn-V DMSs is whether inter-Mn exchange (and hence T_C) changes monotonically across the Ga-based pnictide series [22-24] from $\text{Ga}_{1-x}\text{Mn}_x\text{Sb}$ (maximum reported T_C 25 K) [8] to $\text{Ga}_{1-x}\text{Mn}_x\text{N}$ (maximum reported T_C 940 K) [25]. The shorter bond length in GaP should lead to greater exchange coupling between holes and Mn ions, which would also imply higher T_C . However, greater exchange coupling would result in more localized hole states with less overlap between different Mn sites which might result in overall weaker inter-Mn exchange. Thus, it may be found that the degree of weak localization in $\text{Ga}_{1-x}\text{Mn}_x\text{As}$ provides a local maximum in the effective inter-Mn exchange strength and hence T_C . Our results indicating a lower T_C for carrier-mediated-based ferromagnetism in $\text{Ga}_{1-x}\text{Mn}_x\text{P}$ do not necessarily suggest that the maximum attainable T_C in this system will also be lower; it is possible that stronger ferromagnetism may be achieved through co-doping with acceptors [14] or further process optimization.

The demonstration of carrier-mediated ferromagnetism in $\text{Ga}_{1-x}\text{Mn}_x\text{P}$ raises new possibilities for the exploration of coupled electrical and magnetic phenomena in DMSs. For example, it was recently predicted that the anomalous Hall coefficient should change sign as the Fermi level changes position within an impurity band [26]. The ability to manipulate both the bandstructure via Mn content and the Fermi energy via compensation in this material makes it an ideal system for experimentally testing such predictions.

In summary, $\text{Ga}_{1-x}\text{Mn}_x\text{P}$ represents a novel DMS alloy system where strongly localized carriers in a detached impurity band stabilize ferromagnetism. The unique electrical, magnetic, and optical properties displayed by this material make it a model system for investigating the rich interplay between bandstructure, carrier localization, and mechanisms of ferromagnetic exchange.

This work was supported by the Director, Office of Science, Office of Basic Energy Sciences, Division of Materials Sciences and Engineering, of the US Department of Energy under Contract No. DE-AC03-76SF00098. The authors thank Y. Suzuki and E.E. Haller for use of characterization facilities, R. Chopdekar and T.W. Olson for experimental assistance, and W. Walukiewicz and K.M. Yu for many fruitful discussions. MAS acknowledges support from an NSF Graduate Research Fellowship. ODD acknowledges support from the Hellman Family Fund.

REFERENCES

1. H. Ohno, A. Shen, F. Matsukura, A. Oiwa, A. Endo, S. Katsumoto, and Y. Iye, Appl. Phys. Lett. **69** (3) 363 (1996).
2. H. Munekata, H. Ohno, S. von Molnar, A. Segmüller, L.L. Chang, and L. Esaki, Phys. Rev. Lett. **63** (17) 1849 (1989).
3. H. Ohno, Science **281** 951 (1998).
4. T. Dietl, Semicond. Sci. Technol. **17** 377 (2002).
5. T. Dietl and H. Ohno, MRS Bul. **28** (10) 714 (2003).
6. F. Matsukura, H. Ohno, and T. Dietl, *Handbook of Magnetic Materials*, Vol. 14, ed. K. H. J. Buschow (Elsevier, Amsterdam, 2002), p. 1.
7. T. Dietl, F. Matsukura, H. Ohno, J. Cibert, and D. Ferrand, to appear in *Proceedings of the NATO Advanced Research Workshop "Recent Trends in Theory of Physical Phenomena in High Magnetic Fields"*, eds. I. Vagner, et al. (Kluwer, Dordrecht, 2003), p. 197.
8. E. Abe, F. Matsukura, H. Yasuda, Y. Ohno, and H. Ohno, Physica E **7** 981 (2000).
9. T. Dietl, H. Ohno, F. Matsukura, J. Cibert, and D. Ferrand, Science **287** 1019 (2000).
10. E.J. Singley, R. Kawakami, D.D. Awschalom, and D.N. Basov, Phys. Rev. Lett. **89** (9) 097203 (2002).
11. B. Clerjaud, J. Phys. C: Solid State Phys. **18** 3615 (1985).
12. L. Kronik, M. Jain, and J.R. Chelikowsky, Appl. Phys. Lett. **85** (11) 2014 (2004).

13. A.J. Blattner and B.W. Wessels, *Appl. Surf. Sci.* **221** 155 (2004).
14. N. Theodoropoulou, A.F. Hebard, M.E. Overberg, C.R. Abernathy, S.J. Pearton, S.N.G. Chu, and R.G. Wilson, *Phys. Rev. Lett.* **89** (10) 107203 (2002).
15. M. A. Scarpulla, O. D. Dubon, K. M. Yu, O. Monteiro, M. R. Pillai, M. J. Aziz, and M. C. Ridgway, *Appl. Phys. Lett.* **82** 1251 (2003).
16. M. A. Scarpulla, U. Daud, K. M. Yu, O. Monteiro, Z. Liliental-Weber, D. Zakharov, W. Walukiewicz, and O. D. Dubon, *Physica B* **340-342**, 908 (2003).
17. M. A. Scarpulla, K. M. Yu, W. Walukiewicz, and O. D. Dubon, <http://arxiv.org/cond-mat/0408021> (2004).
18. M. A. Scarpulla, R.C. Petroski, K. M. Yu, D. Zakharov, O. Monteiro, Z. Liliental-Weber, M. J. Aziz, and O.D. Dubon, in preparation.
19. K.Y. Wang, R.P. Champion, K.W. Edmonds, M. Sawicki, T. Dietl, C.T. Foxon, and B.L. Gallagher, <http://arxiv.org/abs/cond-mat/0411475>.
20. M. Viret, L. Ranno, and J.M.D. Coey, *Phys. Rev. B* **55** (13) 8067 (1997).
21. E. A. Davis and W. D. Compton, *Phys. Rev.* **140** (6A) 2183 (1965).
22. P. Mahadevan and A. Zunger, *Appl. Phys. Lett.* **85** (14) 2860 (2004).
23. K. Sato, P.H. Dederichs, H. Katayama-Yoshida, J. Kudrnovsky, *J. Magn. Magn. Mater.* **272-276** 1983 (2004).
24. T. Jungwirth, J. Konig, J. Sinova, J. Kucera, and A.H. MacDonald, *Phys. Rev. B* **66** (1) 012402 (2002).

25. T. Sasaki, S. Sonoda, Y. Yamamoto, K. Suga, S. Shimizu, K. Kindo, H. Hori, *J. Appl. Phys.* **91** 7911 (2002).
26. A.A. Burkov and L. Balents, *Phys. Rev. Lett.* **91** (5) 057202 (2003).

FIGURE CAPTIONS

Figure 1 – Low-field (50 Oe) magnetization as a function of temperature for a $\text{Ga}_{0.94}\text{Mn}_{0.06}\text{P}$ film and a sample compensated with Te. The nearly linear magnetization is characteristic of ferromagnetic III-V semiconductors near a metal-insulator transition [17].

Figure 2 – Hall resistance as a function of field [main] and magnetoresistivity at 7 T as a function of temperature [inset] for the sample of $\text{Ga}_{0.94}\text{Mn}_{0.06}\text{P}$. The Hall data at 100 K are fit with a Brillouin function assuming $3.5 \mu_B$ per substitutional Mn.

Figure 3 – Sheet resistivity as a function of inverse temperature for $\text{Ga}_{0.94}\text{Mn}_{0.06}\text{P}$. The black line shows the fit to the model described in the text and gives the high-temperature activation energy as 31 meV and the low-temperature activation energy as 6 meV.

Figure 4 - (a) Far IR photoconductive response from the $\text{Ga}_{0.94}\text{Mn}_{0.06}\text{P}$ sample (solid) and instrument response (dashed) showing the 26 meV optical gap. (b) Far IR photoconductive response from the Te compensated sample showing thermal redistribution of holes as temperature increases. (c) 10 K IR absorption from a Te compensated sample. The peak centered near 400 meV is due to the Mn impurity band. (d) Schematic density of states showing the Mn band separated from the valence band by an energy gap. The bottom two portions of the figure are enlarged views of the region near the gap in the Mn only and Te compensated cases. Each depicts a photoexcited hole

transition: in the Te compensated case, the transition energy is larger as a result of the increased Fermi energy (E_F).

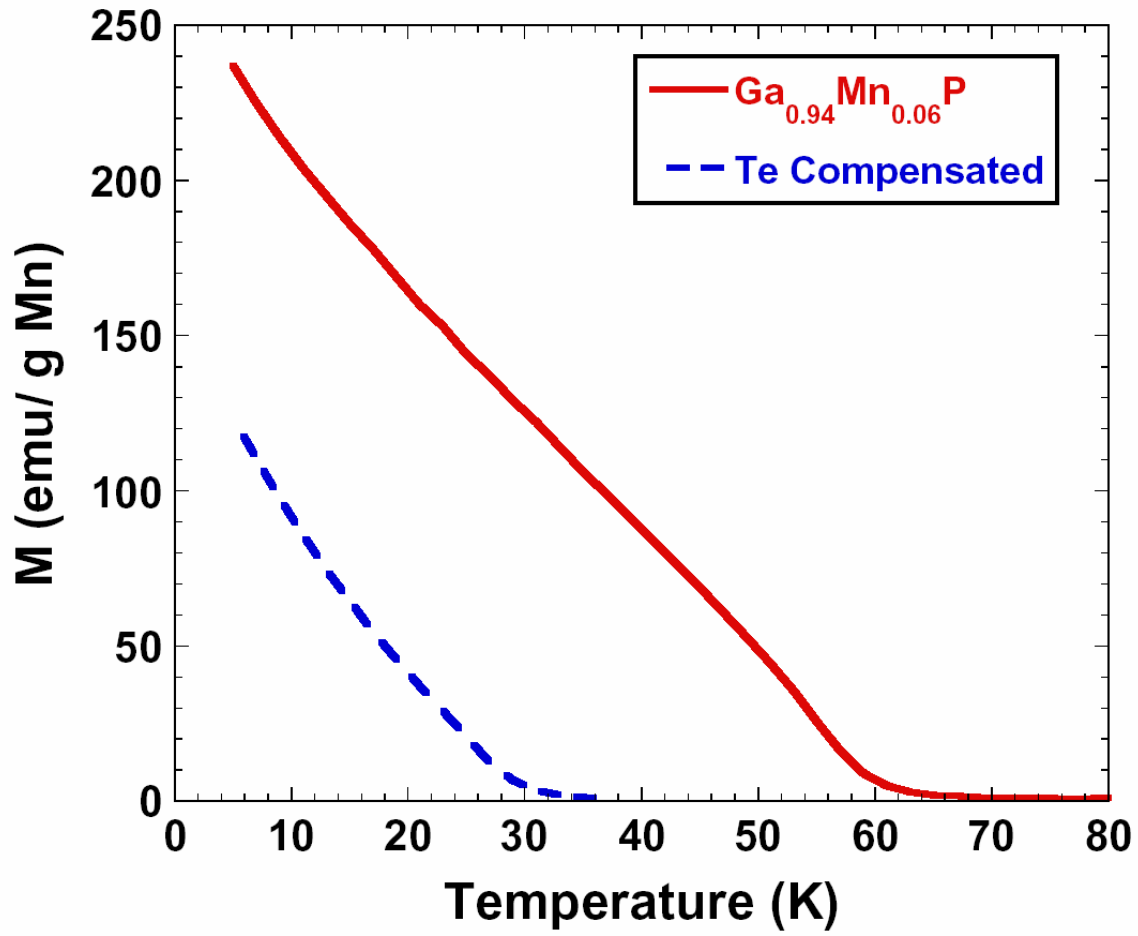


FIGURE 1

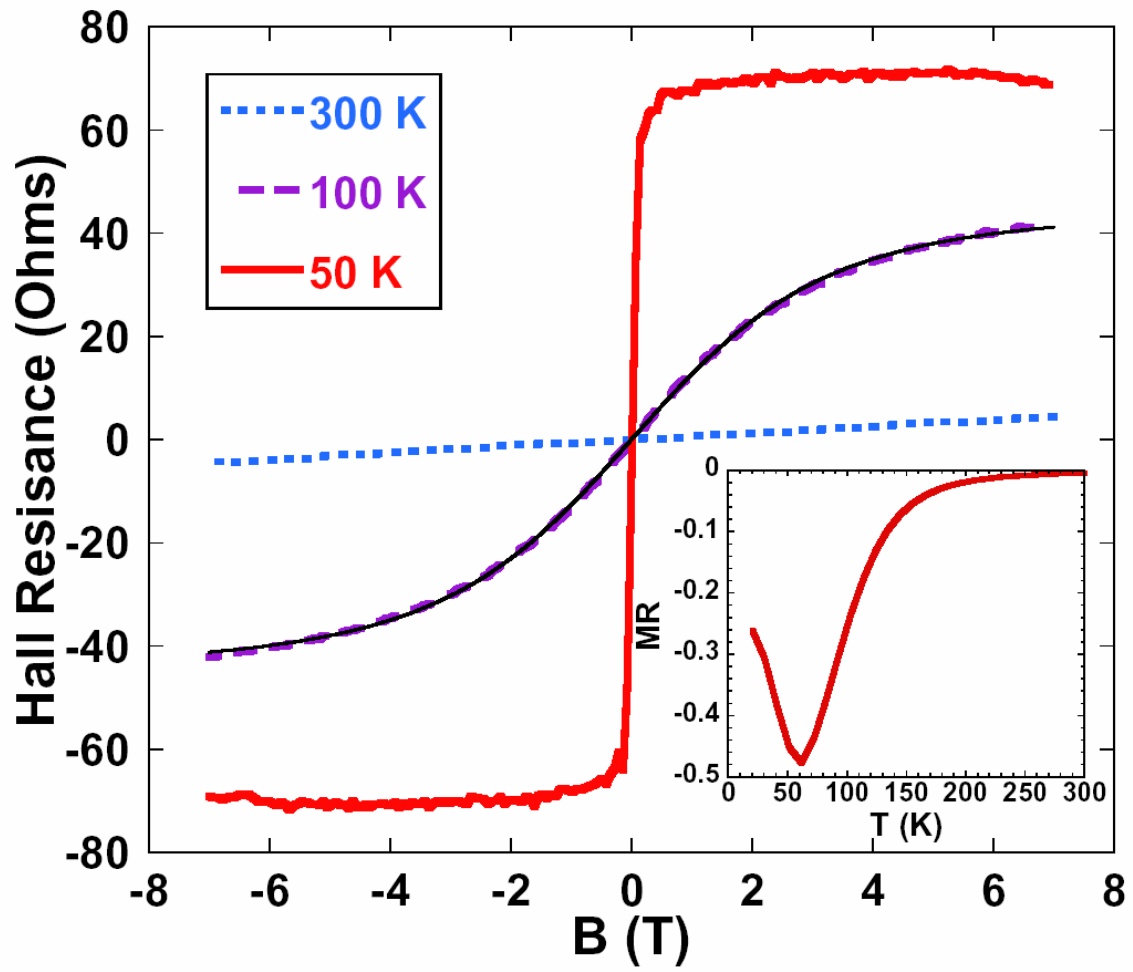


FIGURE 2

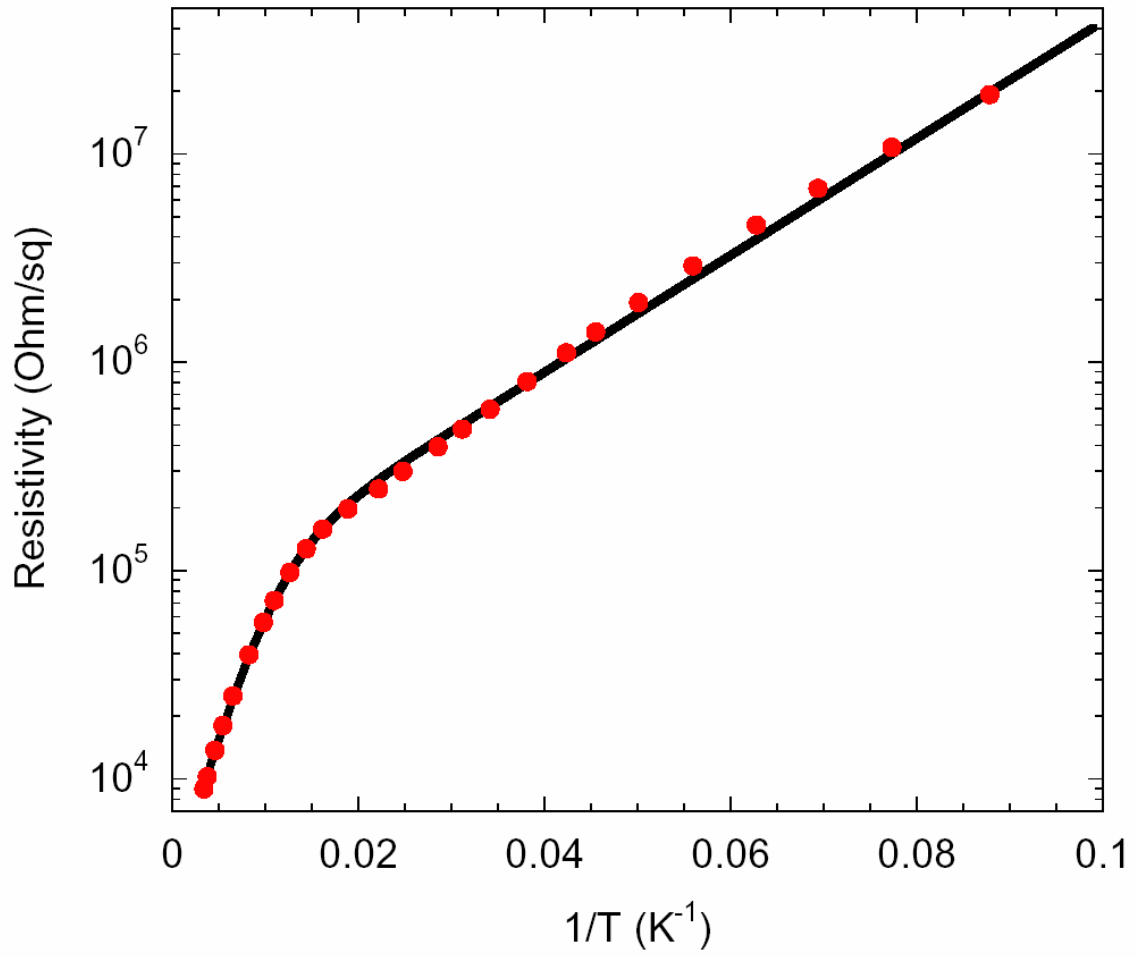


FIGURE 3

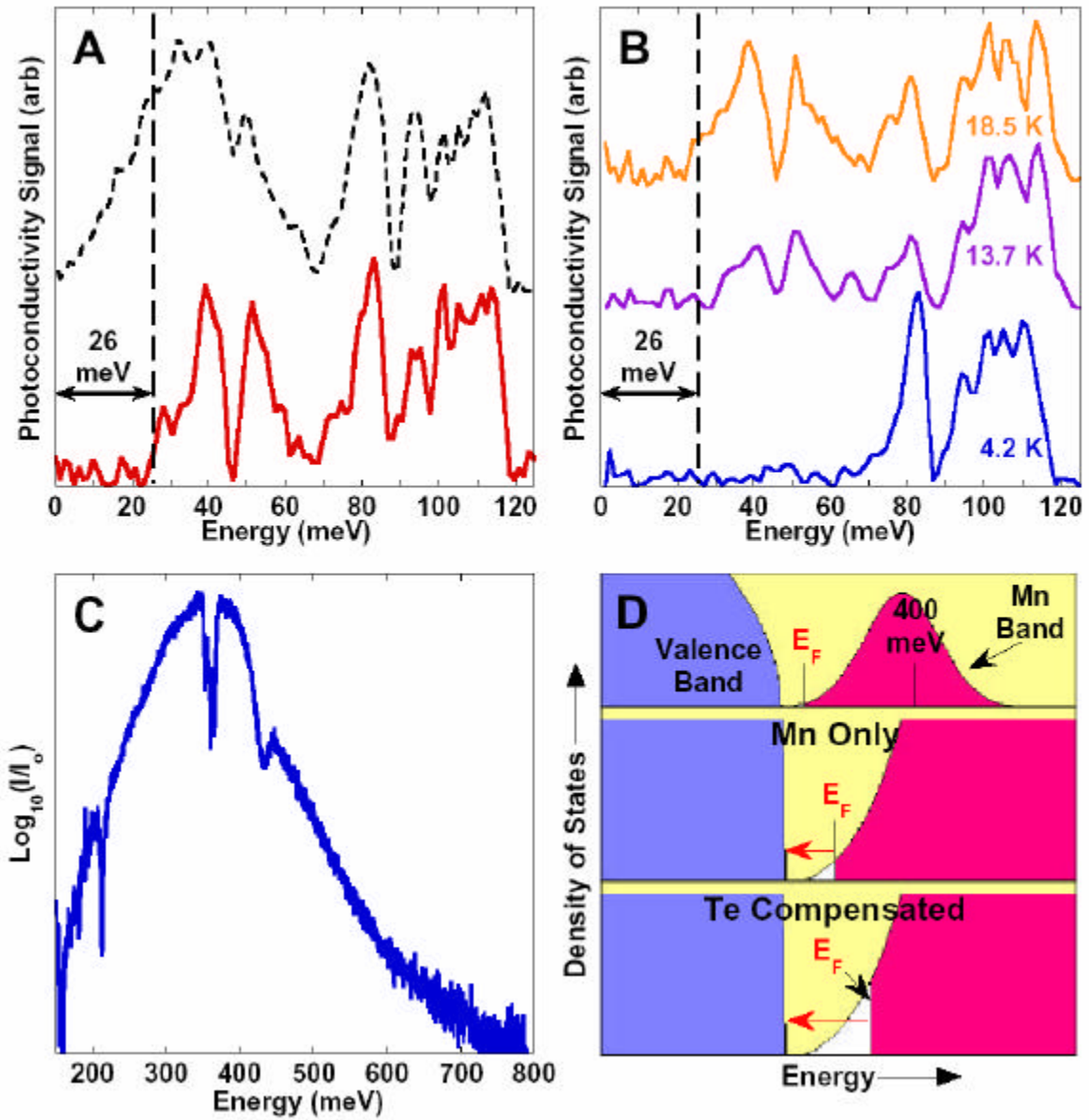


FIGURE 4